Review

On Case-Fatality Rate: Review and Hypothesis

Hiroshi Yoshikura*

National Institute of Infectious Diseases, Tokyo 162-8640, Japan

CONTENTS:

SUMMARY: The relationship between log cumulative number of patients (X) and that of deaths (Y) in an epidemic follows the equation $\log Y = k\log X - k\log N_0$, where k is a constant determining the slope and N_0 is the value of X when Y = 1. Diseases with k = 1 are Ebola hemorrhagic fever, avian influenza H5N1, cholera, and hand, foot, and mouth disease; those with k > 1 are the influenza H1N1 2009 pandemic in countries other than Mexico and the SARS epidemic in some countries; and those with k < 1 include the influenza H1N1 2009 pandemic in Mexico. Epidemics with k > 1 can be simulated by postulating two subpopulations (normal population [NP] and vulnerable population [VP]), where the epidemic proceeds at higher speed and at higher mortality in VP than in NP. Epidemics with k < 1 can be simulated by postulating coexisting <u>h</u>igh <u>v</u>irulence <u>v</u>irus (HVV) and <u>l</u>ow <u>v</u>irulence <u>v</u>irus (LVV), with the former being propagated at slower speed and with a higher mortality rate than the latter. An epidemic with k > 1 was simulated using parameters that are fractions of subpopulations NP or VP from the total population (f) and NP- or VP-specific patient multiplication (M) and mortality (D) rates. An epidemic with k < 1 was simulated using parameters that are fractions of HVV- or LVV-infected human populations (f), and HVV- or LVV-specific M and D.

1. Introduction

The case fatality rate is "a measure of disease severity and is defined as the proportion of patients with a specified disease or condition who die within a specified time" (1) or "as the percentage of the number of persons diagnosed as having a specific disease who die as a result of that illness. This term is most frequently applied to a specific outbreak of acute disease in which all patients have been followed for an adequate period of time to include all attributable deaths" (2). Though these definitions acknowledge that case-fatality rate is not independent of time of observation, by using a qualification such as "within a specific time" or "adequate period of time," the rate has been treated as constant in most textbooks and in the modeling of epidemics.

A series of my work (3–6), however, has shown that for some epidemics, the case-fatality rate thus defined changes over time. This article briefly summarizes my previous work on this topic and further explores how different factors affect the dynamics of the case-fatality rate.

2. Review of previous observations

In March 2009, the novel influenza 2009 H1N1 pandemic was first reported in Mexico and in the southwestern part of the USA. Figure 1 shows the time course of cumulative number (expressed in logarithm) of patients (Fig. 1A) and that of the cumulative number of deaths (Fig. 1B) from the epidemics in Mexico, the USA, and Argentina (data source: http://idsc.nih.go.jp/disease/swine_influenza/wcases01.html [in Japanese]). The curves of cumulative numbers of patients in Mexico and in the USA were almost overlapping in the first 20 days (from April 30 to May 22), and then the curve for the USA continued to rise while that of Mexico faltered. In Argentina, the number of patients started to increase with a lag of ~30 days with kinetics similar to those of the USA. The cumulative number of deaths in Mexico increased in parallel with the increase in the number of patients, while in the USA and Argentina the kinetics more closely represented an exponential increase.

In Fig. 2A, the plots in Figs. 2A and 2B were combined by eliminating the common parameter of time to make log-log plots. The plots followed the equation $\log Y = k\log X - k\log N_0$, where k is a constant deter-

*Corresponding author: Mailing address: Department of Food Safety, Ministry of Health, Labour and Welfare, 1-2-2, Kasumigaseki, Chiyoda-ku, Tokyo 100-8916, Japan. Tel: +81-3-3595-2326, Fax: +81-3-3503-7965, E-mail: yoshikura-hiroshi@mhlw.go.jp
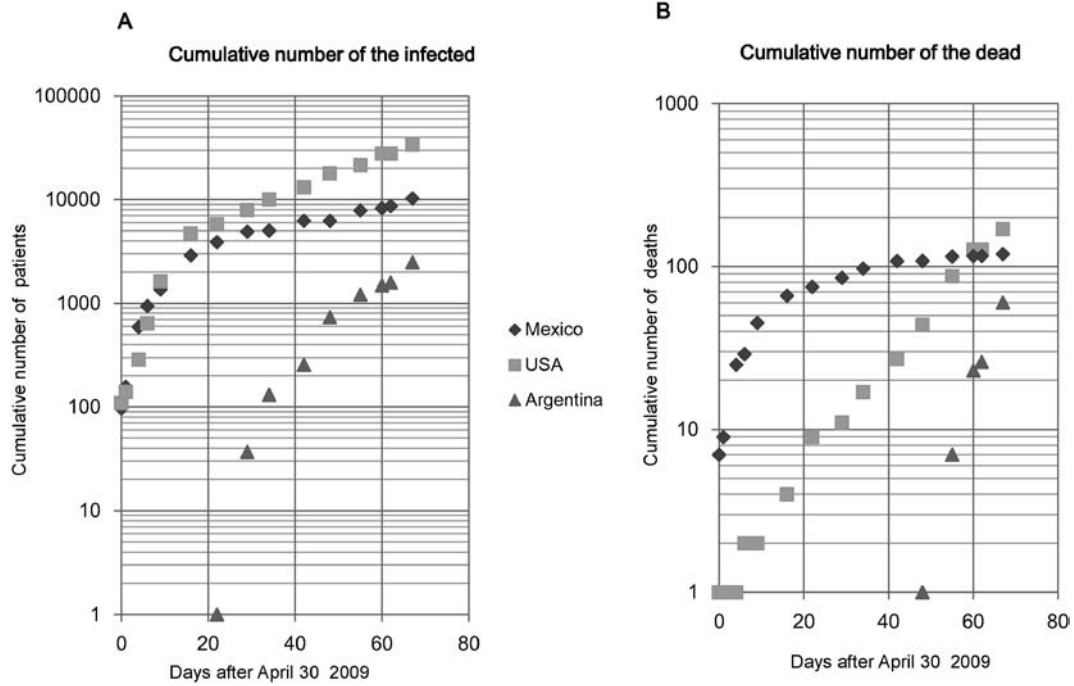
Fig. 1. Time course of cumulative number of patients (A) and cumulative number of deaths (B) in 2009 H1N1 Pandemic (April 30–July 6, 2009). The vertical axis shows the cumulative number of patients (A) or that of deaths (B). The horizontal axis shows number of days after April 30, 2009.
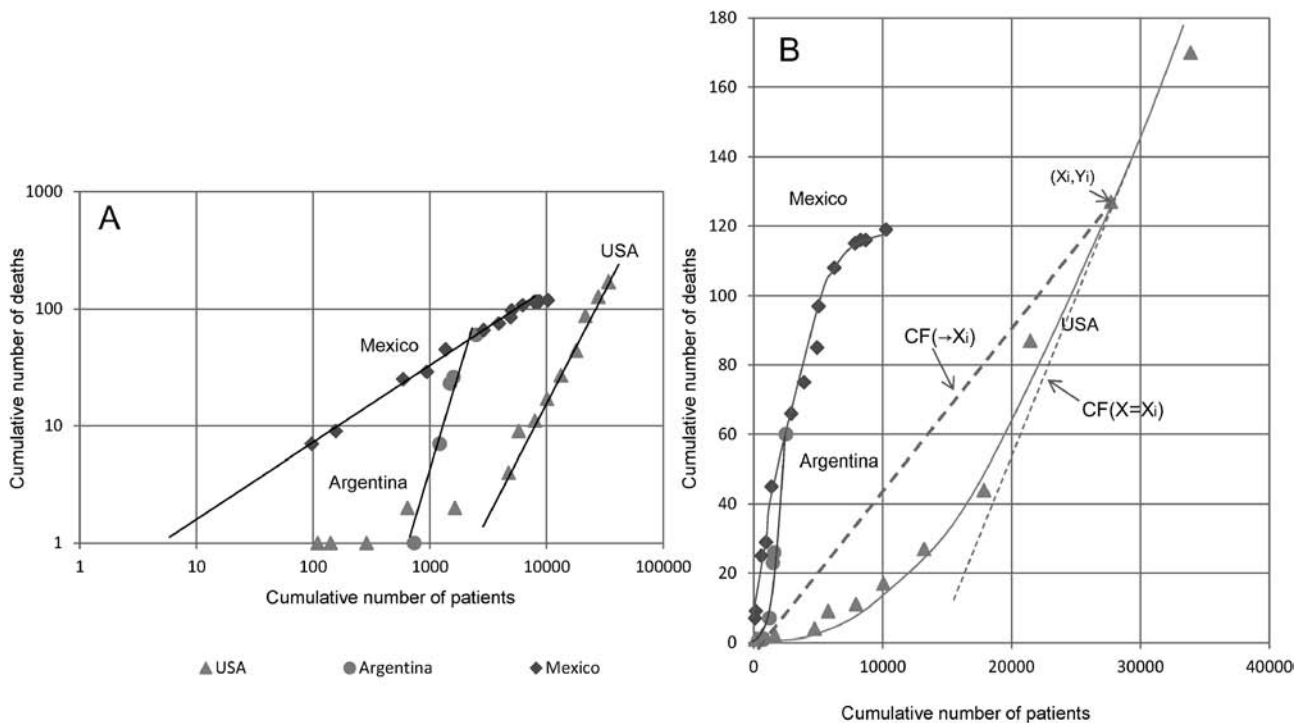

Fig. 2. Plot of cumulative number of deaths versus cumulative number of patients. (A) Log-log plot reproduced from the previous publication (3). (B) Plot in the ordinary scale. The slope of CF($\rightarrow X_i$) and that of CF($X = X_i$) are shown by broken lines.

mining the slope, and N_0 is the value of X when Y = 1 or the cumulative number of patients when the first death appeared. The slope of the plot for Mexico was $< 45°$ (k = 0.65) and that of Argentina and the USA was $> 45°$ (k = 2.8 for Argentina and ~ 1.8 for the USA) (3). In appearance, the case-fatality rate continu-ously decreased in Mexico and continuously increased in Argentina and in the USA. Figure 2B shows the same plot in the normal scale. The curves for Argentina and the USA were concave, while that for Mexico was con-vex (note that these plots cannot be approximated prop-erly by drawing regression lines crossing the origin of
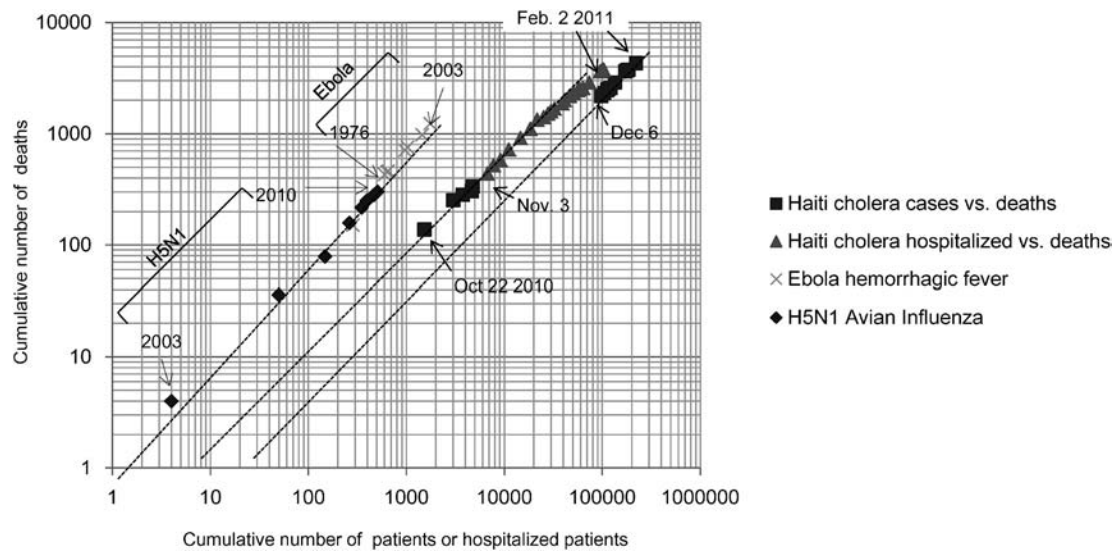
Fig. 3. The log-log plot for Ebola hemorrhagic fever (1976–2003), avian influenza H5N1 (2003–2010), and the cholera epidemic in Haiti (October 22, 2010–February 2, 2011). For Ebola hemorrhagic fever and avian influenza H5N1, the plots are on a yearly basis. The vertical axis shows the cumulative number of deaths and the horizontal axis that of the patients.

the coordinates). The curves can be expressed through transformation of $\log Y = k \log X - k \log N_0$, as $Y = X^k/N_0^k$. The case-fatality rate (CF) calculated for the period that elapses from the start of an epidemic to the point $X = X_i$, is expressed as $CF(\to X_i) = Y_i/X_i = X_i^{k-1}/N_0^k$. The temporal CF at X_i, $CF(X = X_i)$, is obtained by differentiating Y with respect to X, i.e., $CF(X = X_i) = (dY/dX)_{X=X_i} = kX_i^{k-1}/N_0^k$. The ratio of $CF(X = X_i)$ to $CF(\to X_i)$ is $(kX_i^{k-1}/N_0^k)/(X_i^{k-1}/N_0^k) = k$. When $k = 1$, $CF(X_i)$ and $CF(\to X_i)$ are both $1/N_0$.

Figure 3 shows the similar log-log plots for total reported cases in the world of Ebola hemorrhagic fever from 1976 to 2003 (http://www.who.int/mediacentre/factsheets/fs103/en/index.html), that of avian influenza H5N1 from 2003 to 2010 (http://www.who.int/csr/disease/avian_influenza/country/cases_table_2011_05_13/en/), and that of the cholera epidemic in Haiti in 2010–2012 (http://new.paho.org/disaster/index.php?option=com_content&task=view&id=1423&Itemid=1). The plots of avian influenza H5N1 and Ebola hemorrhagic fever had slopes of 45° (i.e., k = 1) with $N_0 \sim 2$, and overlapped each other, indicating that the two epidemics are similar in nature with high and constant case-fatality rates over time.

For the cholera epidemic in Haiti, the World Health Organization (WHO) website gives, in addition to number of deaths, number of cases from October 22 to 30, 2010, number of hospitalizations from November 3 to December 1, and the number of cases and number of hospitalized from December 6, 2010 to January 9, 2011. The plot of cases versus deaths (October 22 to 30) and hospitalized patients versus deaths (November 3 to December 1) were overlapping. From December 6 to January 9 of the next year, the plot of deaths versus cases shifted horizontally to the right, and that of deaths versus hospitalized curved slightly to the right. The shift that occurred from late November to early December in 2010 was probably brought about by improved care of patients through international aid. N_0 before the shift

Table 1. Classification of epidemics according to k > 1, k = 1, or k < 1

Slope	Epidemic
k > 1	SARS in Hong Kong[1] and Singapore (6); influenza H1N1 2009 pandemic in Argentina, USA, and Canada (3); influenza H1N1 2009 pandemic in AFRO, EURO[2], SEARO, EMRO, and WPRO[2] (5)
k = 1	SARS in Canada, China, and Taiwan (6), Cholera in Haiti in 2010/2011 (6 and this article); Hand, foot, and mouth disease in China 2008–2010; Ebola (this article); Avian influenza H5N1 (this article)
k < 1	influenza H1N1 2009 pandemic in Mexico (3)

[1]: Initial rise with k = 1 followed by the curve with k > 1.
[2]: Initial long steep rise followed by less steep rise.

was ∼8, while it was 30 after the shift, which corresponds to reduction of the case-fatality rate from ∼13% to 3.3%, about a 4-fold reduction.

Table 1 classifies the epidemics so far examined according to the slope of the log-log plot. While case-fatality rate was constant or near constant in avian influenza H5N1, Ebola hemorrhagic fever, the 2010 cholera epidemic in Haiti, and hand, foot, and mouth disease (HFMD) in China (5), this was clearly not so in the influenza 2009 H1N1 pandemic (3,5) and in some severe acute respiratory syndrome (SARS) epidemics (6).

3. How can case-fatality rate change over time during an epidemic if mortality rate is specific to each pathogen-host pair?

The mortality rate is determined by the balance between the pathogen virulence and the host defense, which is expected to be specific to any pathogen-host pair. If case-fatality rate changes over time, it should be due to changes in the pathogen-host pairs. How can such a situation occur in a single epidemic? It can occur only when multiple host-pathogen combinations exist,
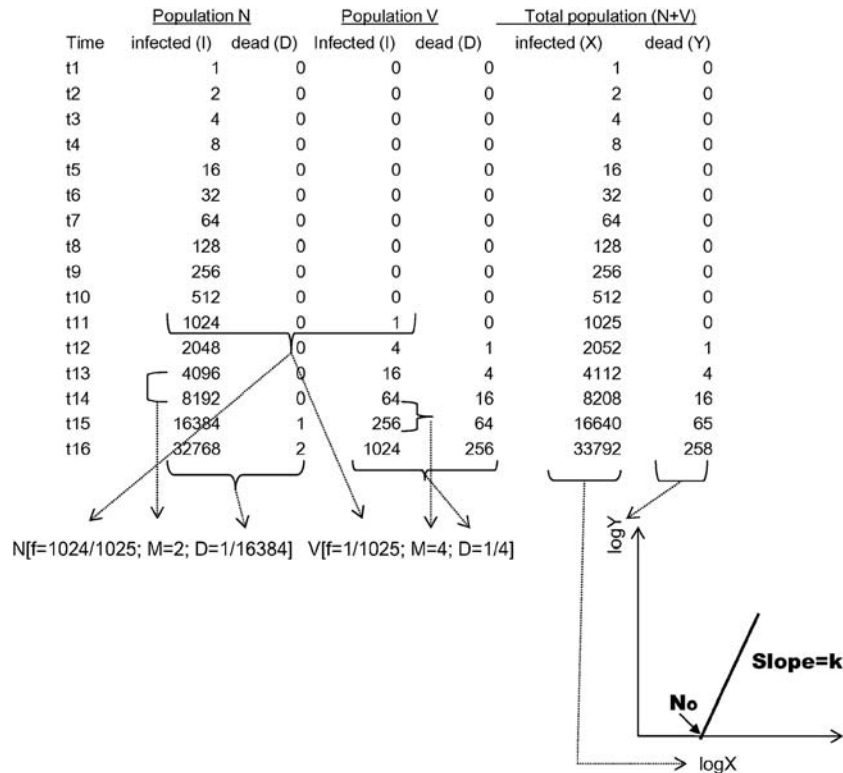
Time	Population N infected (I)	Population N dead (D)	Population V Infected (I)	Population V dead (D)	Total population (N+V) infected (X)	Total population (N+V) dead (Y)
t1	1	0	0	0	1	0
t2	2	0	0	0	2	0
t3	4	0	0	0	4	0
t4	8	0	0	0	8	0
t5	16	0	0	0	16	0
t6	32	0	0	0	32	0
t7	64	0	0	0	64	0
t8	128	0	0	0	128	0
t9	256	0	0	0	256	0
t10	512	0	0	0	512	0
t11	1024	0	1	0	1025	0
t12	2048	0	4	1	2052	1
t13	4096	0	16	4	4112	4
t14	8192	0	64	16	8208	16
t15	16384	1	256	64	16640	65
t16	32768	2	1024	256	33792	258

N[f=1024/1025; M=2; D=1/16384] V[f=1/1025; M=4; D=1/4]

logY

Slope=k

No

logX

Fig. 4. Table format used for simulation of epidemics. See text. Microsoft Office Excel 2007 was used for all data processing and graphics.

N[M=2, D=1/1024]
V[M=4, D=1/4]
N[f=512/513, M=2, D=1/1024], V[f=1/513, M=4, D=1/4]

N[M=4; D=1/1024]
V[M=2; D=1/4]
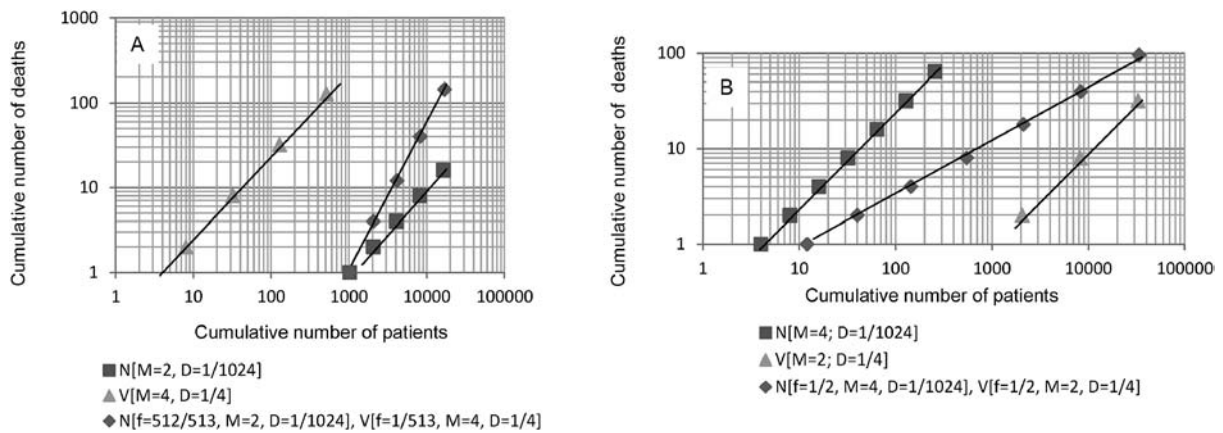N[f=1/2, M=4, D=1/1024], V[f=1/2, M=2, D=1/4]

Fig. 5. Derivation of the log-log plot of composite populations of normal population (NP) and vulnerable population (VP). (A) shows simulations of curves with k > 1, where the ratio of the patients in NP and those in VP was 512:1 when the first patient appeared in VP. (B) shows the simulations of curves with k < 1, where the ratio of the patients in population NP and those in population VP was 1:1 at time t_1. Note the log-log plot for component subpopulations NP and VP (in squares and triangles, respectively) gives a straight line with the slope of 45°. The vertical axis shows the cumulative number of the deaths and the horizontal axis that of the patients.

i.e., when the human population consists of subpopulations with different susceptibilities or the pathogens consisting of subpopulations differing in virulence.

Figure 4 shows the principle of tabulating such a hypothetical epidemic. The left-most column shows the time elapsed (the time interval from time t_i to time t_{i+1} is not necessarily constant in terms of physical time, as the speed of spread of a pathogen may not be constant during an epidemic). The second and the third columns, respectively, show cumulative numbers of patients and deaths in the normal population (NP). The fourth and fifth columns, respectively, show those in the vulnerable population (VP). The sixth and seventh columns, respectively, show those for the whole population, which were obtained by adding the respective numbers of NP and VP, i.e., $X = I_{(NP)} + I_{(VP)}$ and $Y = D_{(NP)} + D_{(VP)}$.

In this model, populations NP and VP are characterized by three parameters: f, M, and D, with f representing the fraction of NP or VP in the total patient population when the first infected case appeared in VP; M being the multiplication factor of the number of patients from t_i to t_{i+1}; and D representing the mortality rate. Thus, for example, a population expressed by N [f = 1,024/1,025; M = 2; D = 1/16,384], V [f =

1/1,025; M = 4; D = 1/4] indicates that there were 1,024 patients in NP versus 1 patient in VP when the first patient appeared in VP; in the unit time interval, the patient number increased by 2-fold in NP and by 4-fold in VP, and the case-fatality rate was 1/16,384 for NP and 1/4 for VP.

Figure 5 shows model plots with k > 1 (Fig. 5A) or k < 1 (Fig. 5B) that were derived from two populations differing in M and D. The plots for the component populations, NP (squares) and VP (triangles), are represented by two lines with 45° slope, and that of total population (NP + VP) by the line (diamonds) in the middle.

As previously indicated (5) and as further discussed in this article, the situation with k > 1 (Fig. 5A) is best simulated by postulating a minor subpopulation, VP, where the infection spreads with a higher mortality rate and at a higher speed than in NP. The situation with k < 1 (Fig. 5B) is best simulated by postulating virus populations consisting of high virulence virus (HVV) and low virulence virus (LVV). LVV spreads in the community at a lower mortality rate and at higher speed than HVV (note that patients infected by a HVV become bedridden and present a reduced chance of further transmission). In the tabulation for k < 1 (Fig. 4), a human population infected with a LVV is coded as NP

and the population infected by HVV as VP.

4. Parameters affecting k and N_0

4–1. Cases with k > 1

A sharp rise after a long latent phase, i.e., k > 1 with large N_0, as observed with the influenza 2009 H1N1 pandemic in Argentina and the USA, means that the epidemic shifted from low case-fatality to increasingly high case-fatality at X = N_0.

In all the simulations with k > 1, D in VP was set significantly higher than in NP. Figure 6 shows the effect of the changes in f, M, and D on the shape of the curve. Figure 6A shows that a slope >45° (i.e., k > 1) can be obtained only when both M and D are higher in VP than in NP. Increasing either M (triangles) or D (diamonds) in population VP alone thus does not result in k > 1 (compare squares with diamonds and triangles). Figure 6B examines the effect of the change in f. When f of VP becomes lower, the curve shifts to the right (compare squares and diamonds). Figure 6C compares the effect on the slope of further increase of M or D in VP. Here, a further increase in M resulted in a steeper slope (compare squares and triangles), while a further increase of D (compare crosses and triangles) shifted the curve to the left but did not change the slope. Thus, M (transmis-
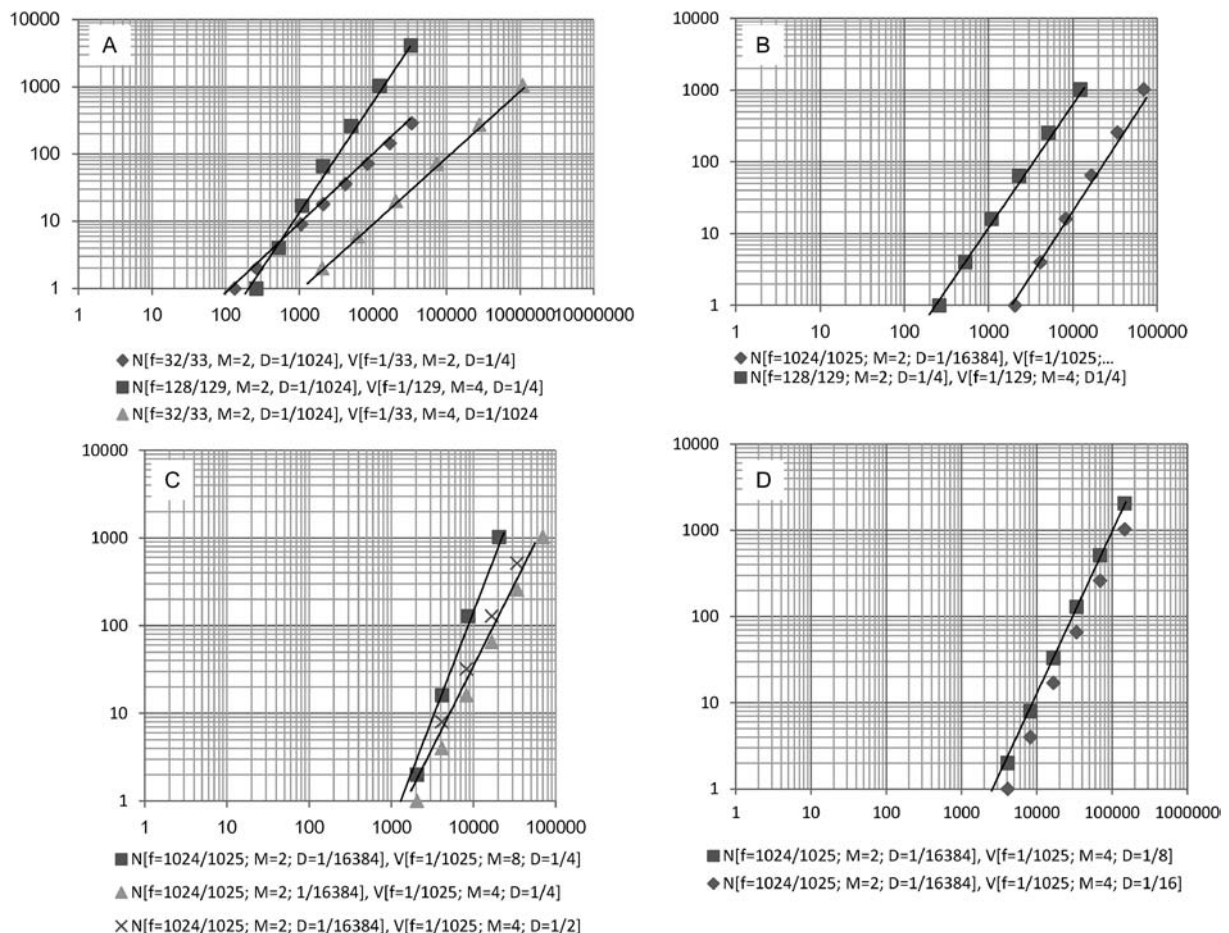

Fig. 6. Simulation for k > 1. (A) examines the effect of M and D on the slope of the log-log plot. The slope becomes >45° only when both M and D are higher in VP than in NP. (B) examines the effect of f on N_0. (C) examines the impact of further increase of M or D in VP on the slope of the log-log plot. (D) shows the simulation of the epidemic in the USA with more realistic parameters, D in NP 1/16,384 and that in VP 1/8 ∼ 1/16. The vertical axis shows the cumulative number of deaths and the horizontal axis that of the patients.
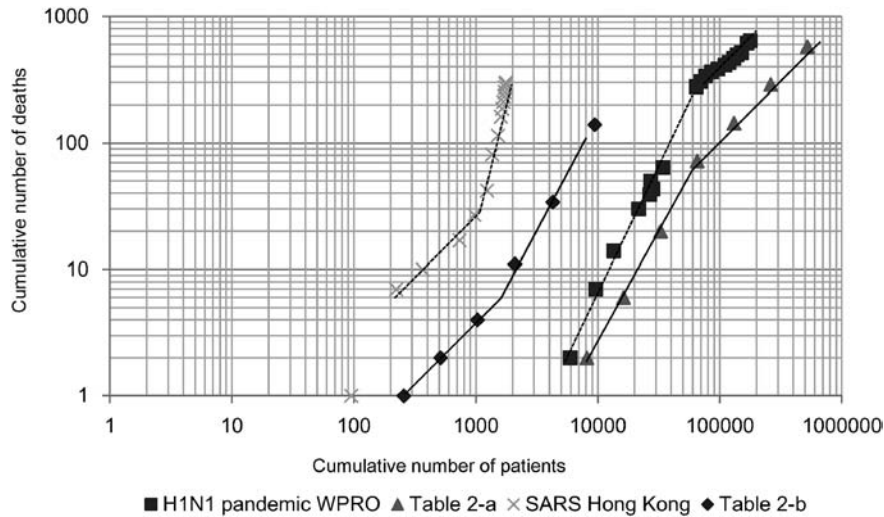
Fig. 7. Simulation of plots with break. See Table 2 for the table used for the plot; Table 2a is for simulation of downward bent and Table 2b for that of upward bent. The vertical axis shows the cumulative number of the deaths and the horizontal axis that of the patients.

Table 2. Tables used for simulation of curves with a break

a

Time (ti)	General population		Variant population		Total population	
	Infected (x)	Deaths (y)	Infected (x')	Deaths (y')	Infected ($x + x'$)	Deaths ($y + y'$)
t1	2	0	0	0	2	0
t2	4	0	0	0	4	0
t3	8	0	0	0	8	0
t4	16	0	0	0	16	0
t5	32	0	0	0	32	0
t6	64	0	0	0	64	0
t7	128	0	0	0	128	0
t8	256	0	0	0	256	0
t9	512	0	0	0	513	0
t10	1024	0	0	0	1028	0
t11	2048	0	0	0	2064	0
t12	4056	0	1	0	4057	0
t13	8112	1	4	1	8116	2
t14	16224	2	16	4	16240	6
t15	32448	4	64	16	32512	20
t16	64896	8	256	64	65152	72
t17	129792	16	512	128	130304	144
t18	259584	32	1024	256	260608	288
t19	519168	64	2048	512	521216	576

sion speed) rather than D (mortality) in VP affects the slope. Figure 6D is a simulation of the plot of the H1N1 2009 pandemic in the USA shown in Fig. 1A. A close approximation was obtained with D = 1/16,384 in NP and D = 1/8 or 16 in VP. These values are within the range of the observed frequency. For example, D for Japan in the H1N1 2009 pandemic estimated by the present method was ~1/60,000 (5) and in a nosocomial pandemic of H1N1 2009, the mortality was 27% (8).

In short, k > 1 requires that both M and D are higher in VP than in NP; further increase of M, but not D, in VP results in a steeper curve; N_0 is mainly determined by f.

Some epidemics were accompanied by upward bent (i.e., the SARS epidemic in Hong Kong) or a downward bent (i.e., the H1N1 2009 pandemic WHO Regional Office for the Western Pacific) (crosses and squares, respectively; Fig. 7). The table used for simulating the upward or downward bent is shown in Table 2. The upward bent was simulated by postulating that an epidemic started in a NP with a relatively high D and then began to involve the VP (diamonds in Fig. 7). The downward bent was simulated by postulating faltering of the transmission speed in VP on account of the population's gradual exhaustion (triangles in Fig. 7). The simulation completed by trials and errors for these types of plots was only partially satisfactory, however. The real situation may not be so simple.

Table 2. Continued

b

Time (ti)	General population		Variant population		Total population	
	Infected (x)	Deaths (y)	Infected (x')	Deaths (y')	Infected ($x + x'$)	Deaths ($y + y'$)
t1	1	0	0	0	1	0
t2	2	0	0	0	2	0
t3	4	0	0	0	4	0
t4	8	0	0	0	8	0
t5	16	0	0	0	16	0
t6	32	0	0	0	32	0
t7	64	0	0	0	64	0
t8	128	0	0	0	128	0
t9	256	1	0		256	1
t10	512	2	1	0	513	2
t11	1024	4	6	0	1030	4
t12	2048	8	36	3	2084	11
t13	4056	16	216	18	4272	34
t14	8112	32	1296	108	9408	140

Table 2a is for simulation of curves with downward bent (i.e., H1N1 2009 pandemic in WPRO). At time t_{16}, M of population VP is switched from 4 to 2 so as to reflect decreasing availability of population VP for transmission (D remains unchanged). Table 2b is for simulation of curves with upward bent (i.e., SARS in Hong Kong). Here, epidemic in population VP starts later than in population NP (t_{10} in population VP contrast to t_1 in population NP) with higher mortality late (1/12 in population VP in contrast to 1/256 in population NP).
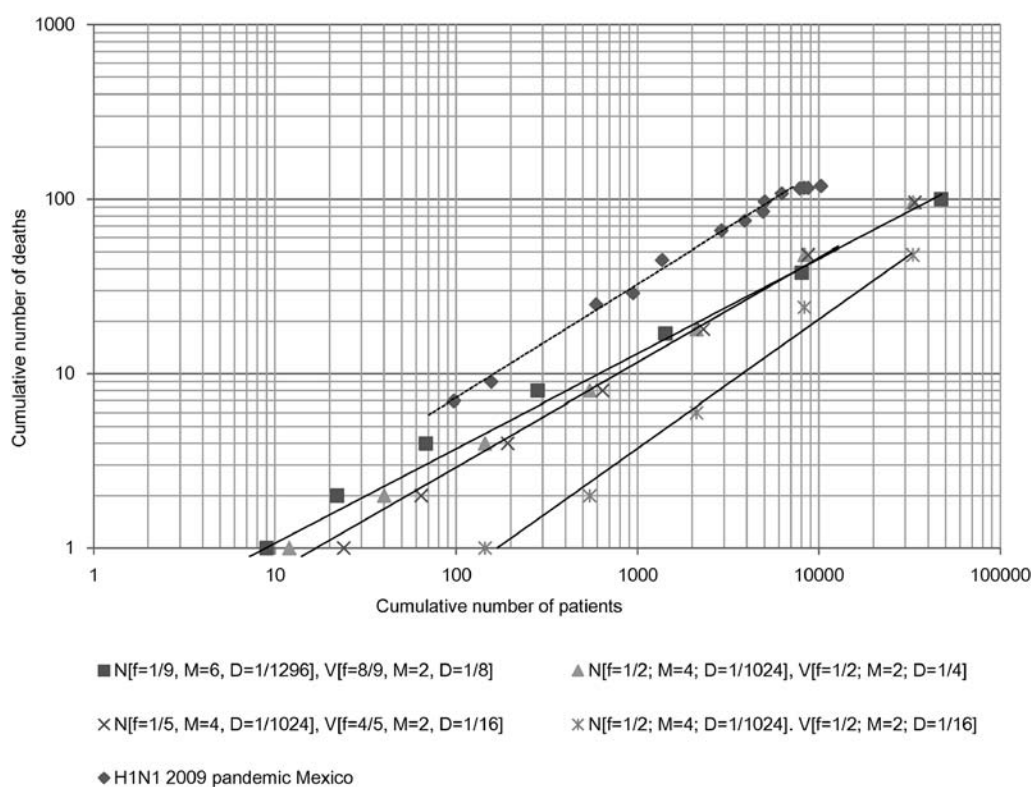

Fig. 8. Simulation for k < 1 appended with the log-log plot of H1N1 2009 pandemic in Mexico. The vertical axis shows the cumulative number of deaths and the horizontal axis that of the patients.

For SARS in Hong Kong and also in mainland China (6), the upward bent can be explained equally well by a scenario in which patients infected towards the end of the epidemic died after cessation of virus spread. It should be remembered, however, that this story does not fit the Singapore SARS epidemic where the log-log plot with k = 3 lasted continuously for 2 months from beginning to end (March 27 to May 30).

4–2. Cases with k < 1

k < 1 occurs when accumulation of deaths with high D lags behind the accumulation of patients. The situation is possible only when mortality rate (D) is higher and virus spread (M) is slower in VP than in NP. In addition, VP has to be sufficiently large so that the deaths in this group represent the deaths of the whole population. Therefore, in the following simulation f was set

1/2 or higher.

Figure 8 examines how f, M, and D influence k and N_0. When f of the VP was increased from 1/2 to 4/5, the plot shifted to the left by 1 log (compare crosses and asterisks). The obtained plot was almost the same as that obtained by increasing D by 4-fold (compare triangles and crosses). This indicates that postulating a population of VP relatively high relative to NP allows a simulation with lower values of D (1/8 ~ 1/16) (see squares and crosses). The plot in the square is a simulation obtained with f = 8/9 and D = 1/8 for VP, in which k was 0.57 and N_0 was ~ 5. These values were not far from the observed values for the Mexican epidemic, k = 0.65 and N_0 = 4 ~ 5 (diamonds; see the plot in Fig. 2A, also).

5. Possible epidemic situations

For k > 1, there are two possible scenarios. One situation arises when the two populations are physically separated. This model fits well to settings such as hospitals, nursing homes, and other facilities housing vulnerable populations where infection spreads easily at a high mortality rate (7).

However, the possibility that k > 1 occurs in mixed populations cannot be entirely excluded. In the mixed population, it is socially active patients in NP who transmit the pathogen to others. As k > 1 occurs at an advanced stage of an epidemic (Fig. 2A), even in the minor VP, the availability of the infection source will not be limiting. Suppose, for example: (i) establishment of infection needs two encounters for normal persons, while a vulnerable person needs only one, and (ii) uninfected persons encounter an infected person at an interval of 3 days. In this case, those belonging to a VP will acquire infection in only 3 days while those belonging to NP need 6 days. Such a scenario could result in a situation where infection spreads at higher speed and at higher mortality among the VP. However, this hypothesis needs confirmation by analytical and/or stochastic mathematical modeling.

For k < 1, the epidemic has to spread at lower speed and at higher mortality in VP than in NP. Let us first examine whether such a situation can be possible with two human subpopulations of different susceptibilities. If subpopulations NP and VP are mixed, the infected persons belonging to NP will mainly spread the virus (because bedridden patients in the VP have fewer opportunities for transmission), and they will do so equally well to persons in NP and VPs. In this situation, while the mortality (D) is higher in VP than in NP, the speed of transmission (M) will be the same for VP and NP. As demonstrated in Fig. 6A, the result is k = 1. The slower spread with high mortality in VP is possible only when VP and NP are physically separated. However, no such situations have been reported from Mexico in the influenza 2009 H1N1 pandemic.

Let us then examine whether k < 1 can be possible when an epidemic is caused by cocirculation of two virus subpopulations, one HVV and the other LVV. While a LVV circulates rapidly with low mortality rate on one hand, the HVV will circulate slowly at a high mortality rate on the other. Such a situation is exactly the one obtained by the simulation shown in Fig. 8,

where the NP is a human population infected by a LVV and the VP is a population infected by HVV.

6. What happened in Mexico in early 2009 and what happened in other countries thereafter?—A hypothesis

Most data so far published have suggested that the case-fatality rate of the novel influenza 2009 H1N1 pandemic was rather low (8–11), which was confirmed by the present author by using the same method described in this paper (5). The reported high mortality in the early epidemic in Mexico has been attributed to the possible low detection rate of the influenza patients (8,9). However, in my view, this claim is not substantiated by direct and/or quantitative data; it is mainly based on backward extrapolation of the later data to the early epidemic in Mexico and/or on some included episodes.

My log-log plot analysis using the raw data (3,4) indicated a different story, i.e., two influenza variants, one highly virulent and one low virulent ones, initiated the influenza 2009 H1N1 pandemic in Mexico, and the low virulence variant took over the epidemic by quickly spreading to the rest of the world. Arguments supporting this hypothesis are as follows. First, there was no anomaly in the data from Mexico. The kinetics of the increase of the cumulative number of cases in Mexico was exactly the same as that in the USA, at least during the first 3 weeks (Fig. 1A), and the kinetics of increase of deaths went in parallel with that of infections, which is quite normal (Fig. 1B). Even if half of the influenza cases in Mexico were not reported, the adjusted kinetics of the cumulative number of patients (Fig. 1A), which shifts by log 2 upward, is almost the same as the original. Second, by transformation of the equation, k is expressed as k = logY/log (X/N_0). The numerator logY (log of number of deaths) usually reflects the reality because death occurs more frequently in hospitals and the cause of most deaths is examined medically. The denominator log (X/N_0) changes little because both X and N_0 are equally affected by the surveillance sensitivity. Therefore, coefficient k is a relatively stable parameter. Third, it is very difficult to conceive that there was such a big difference in disease surveillance as claimed (8,9) between Mexico and other countries in Central and South America. Fourth, though it may be argued that k < 1 is attributable to improved medical intervention made after the outbreak, this argument cannot be supported by the simulation in Fig. 6C or the data on the cholera epidemic in Haiti (Fig. 3), which showed that a change in mortality rate (D) hardly affects the slope of the curve (k) and only shifts the plot horizontally.

Considering the intrinsic high mutability of the influenza virus, LVVs may easily arise through mutation from HVVs. LVVs will soon overwhelm HVVs on account of spreading transmission advantage and the capacity to immunize the population against the slowly spreading HVVs. The detection of multiple genetic groups among the 2009 H1N1 pandemic isolates (10) indicates the high mutability of the virus and its antigenic homogeneity (10) allows the less virulent strains to act as a natural live vaccine.

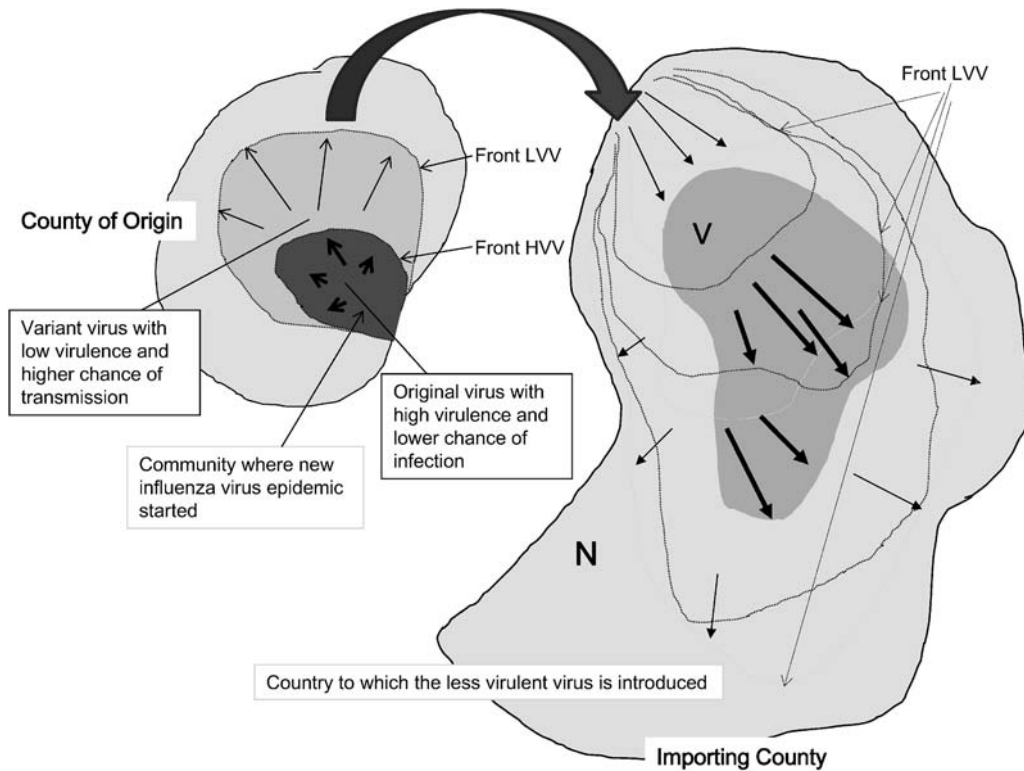If this hypothesis is confirmed, a highly virulent

Fig. 9. Possible model of influenza H1N1 2009 pandemic. The left graphic represents Mexico and the right side the rest of the countries in the world. In Mexico the epidemic started locally and expanded to the whole country. There, the less virulent variant, LVV (line marked as front LVV) spreads ahead of the original virulent strain, HVV (line marked as front HVV), while immunizing the whole population against the virulent strain (left graphic). It is the less virulent strain that was exported to the rest of the world (right graphic). N, NP; V, VP.

strain should have been isolated already, but the isolates from 2009 H1N1 pandemic had no markers associated with high pathogenicity (12). However, there are suggestive footprints of such isolates. The isolates from some severe cases had a D225G mutation that confers dual binding specificity enabling infection to the lower respiratory tract, and one particular plaque isolate had highly increased lethality to mice (13). One of the first US isolates was characterized by increased replication and pathological changes in the lungs of nonhuman primates (14). The high animal pathogenicity exhibited by these different isolates is compatible with a hypothesis that the originating virus had genetic trait conferring a high virulence.

The hypothesis appears to be supported also by the early clinical accounts. ''In contrast to seasonal influenza, most serious illnesses have occurred among children and non-elderly adults,'' and ''approximately one quarter to one half who were hospitalized or died had no reported coexisting medical conditions'' (10). Reporting their experience in Mexico, Dominguez-Cherit et al. noted that among 899 patients admitted for severe pneumonia, 58 were critically ill and 24 of them died within 60 days; the mean age was 44 years (15). Similarly, Chowell et al. reported that among 2,155 patients with severe pneumonia, 821 were admitted and 100 among them died. Seventy-one percent of the severe pneumonia cases were patients 5–59 years old (16). A similar observation was made by Perez-Padilla et al. (17).

Figure 9 is the summary diagram showing what may

have happened during the influenza H1N1 2009 pandemic starting from its origin in Mexico (left graphic) to the rest of the world (right graphic).

7. Some additional remarks

It should be noted that the parameter N [f;M;D], V [f;M;D] was not obtained through mathematical treatment of the equation. It was obtained by trial and error. The solutions presented may not be the only solutions. In fact, the different combinations of f, M, and D gave similar plots (Fig. 8). To obtain a more concrete picture of epidemics with different parameters, mathematical modeling is necessary. Whether $k > 1$ occurs in the mixed population or not needs such a treatment.

Epidemics can be largely divided into those with $k = 1$ and those with $k \neq 1$. Ebola hemorrhagic fever, avian influenza H5N1, cholera, and HFMD belong to the former, and influenza H1N1 2009 pandemic and SARS belong to the latter. The first group includes infections with extremely high mortality, such as Ebola hemorrhagic fever and avian H5N1 influenza, which are less likely to cause a large outbreak, and fecal-oral infections, such as HFMD and cholera, which expose all the populations equally even though the mortality rate may differ among subpopulations (recall that $k > 1$ requires that both M and D are higher in the VP than in the NP). The second group, including the influenza H1N1 2009 pandemic and SARS, is characterized by airborne or droplet transmission requiring relatively close human contacts, high transmission rates, influence of host

factors on severity, and probably the influence of local social structure on the transmission pattern.

What is the implication of the present study on the epidemic potential of avian influenza H5N1? My guess is that the situation could become very similar to the influenza H1N1 2009 pandemic, though it will cause more fatalities by infecting all age groups because there no immunity obtained by the past epidemics. So long as it remains in the avian community, H5N1 will remain a local fatal infection as Ebola hemorrhagic fever has. Once it gets into a human community, an epidemic will start with high mortality rate, as in Mexico in 2009, which will be followed by extremely rapid propagation of less virulent variants. However, if the community where the virus is first introduced allows easy virus transmission, such as a crowded impoverished community without sufficient medical care, selection for attenuated variants will be insufficient and strain(s) with relatively high virulence may be released into the outer world as epidemic strain(s).

Policy implications derived from the above analysis are the following. First, avian H5N1 introduced into human communities has to be detected and contained as quickly as possible. Second, once it starts to propagate, the chance of transmission should be reduced to the minimum so as to select against HVV. In these regards, the government of Mexico should be praised for the early detection of the H1N1 pandemic in 2009 and WHO for its due reaction, which has sometimes been criticized as overplay. Third, when a highly infectious but less virulent virus becomes the main epidemic strain (detected by high N_0 and $k > 1$), the target of hygienic and clinical measures can be shifted from the general public to VP, such as, hospitals, dispensaries, nursery schools, etc.

The influenza H1N1 2009 pandemic showed the utility of faithful documentation of the early epidemic and the importance of early virus isolation. The information thus obtained will be of immense value for assessing the risk of the next influenza pandemic, which could be more serious than the present H1N1 2009 pandemic.

Conflict of interest None to declare.

REFERENCES

1. Bonita, R., Beaglehole, R. and Kjellstrom, T. (2006): Basic Epidemiology. 2nd ed. World Health Organization.
2. Benenson, A.S. (ed.) (1990): Control of Communicable Diseases in Man. 15th ed. American Public Health Association.
3. Yoshikura, H. (2009): Two parameters characterizing 2009 H1N1 swine influenza epidemic in different countries/regions of the world. Jpn. J. Infect. Dis., 62, 411–412.
4. Yoshikura, H. (2009): Two-population model accounting for the different patterns observed in the log-log plot of the cumulative numbers of those infected and killed in the early phase of the 2009 H1N1 pandemic in contrast to the one-population model accounting for the 1918–1919 pandemic in San Francisco. Jpn. J. Infect. Dis., 62, 482–484.
5. Yoshikura, H. (2010): Common features of 2009 H1N1 influenza pandemic in different parts of the world revealed by log-log plot of the cumulative numbers of infected and deceased cases. Jpn. J. Infect. Dis., 63, 148–149.
6. Yoshikura, H. (2011): A new method for monitoring and forecasting the case-fatality rate in ongoing epidemics and its evaluation using published data of SARS in 2003, H1N1 pandemic in 2009/2010, hand-foot-mouth disease in China in 2009/2010, and cholera in Haiti in 2010. Jpn. J. Infect. Dis., 64, 92–94.
7. Enstone, J.E., Myles, P.R.M., Openshaw, P.J.M., et al. (2011): Nosocomial pandemic (H1N1) 2009, United Kingdom, 2009–2010. Emerg. Infect. Dis., 17, 592–598.
8. Wilson, N. and Baker, M.G. (2009): The emerging influenza pandemic: estimating the case fatality ratio. Eurosurveillance, 14, 1–4.
9. Fraser, C., Donnelly, C.A., Cauchemez, S., et al. (2009): The WHO Rapid Pandemic Assessment Collaboration. Pandemic potential of a strain of influenza A (H1N1): early findings. Science, 324, 1557–1561.
10. Writing Committee of the WHO Consultation on Clinical Aspects of Pandemic (H1N1) 2009 Influenza (2010): Clinical aspects of pandemic 2009 influenza A(H1N1) virus infection. N. Engl. J. Med., 362, 1708–1719.
11. Kamigaki, T. and Oshitani, H. (2009): Epidemiologica; characteristics and low case fatality rate of pandemic (H1N1) 2009 in Japan. PLoS Curr. 2009 Dec 20; 1:PRN1139.
12. Neuman, G., Noda, T. and Kawaoka, Y. (2009): Emergence and pandemic potential of swine-origin H1N1 influenza virus. Nature, 459, 931–939.
13. Zheng, B., Chan, K.H., Zhang, A.J.X., et al. (2010): D225G mutation in hemmagglutinin of pandemic influenza H1N1 (2009) virus enhances virulence in mice. Exp. Biol. Med., 235, 981–988.
14. Itoh, Y., Shinya, K., Kiso, M., et al. (2009): In vitro and in vivo characterization of new swine-origin H1N1 influenza viruses. Nature, 460, 1021–1025.
15. Dominguez-Cherit, G., Lapinsky, S.E., Macias A., et al. (2009): Critically ill patients with 2009 influenza A(H1N1) in Mexico. JAMA, 302, 1880–1887.
16. Chowell, G., Bertozzi, S.M., Colcherto, M.A., et al. (2009): Severe respiratory disease concurrent with the circulation of H1N1 influenza. N. Engl. J. Med., 361, 674–679.
17. Perez-Padilla, R., de la Rosa-Zamboni, D., Ponce de Leon, S., et al. (2009): INER Working Group on Influenza. Pneumonia and respiratory failure from swine-origin influenza A(H1N1) in Mexico. N. Engl. J. Med., 361, 680–689.